Cell

Membrane Binding by tBid Initiates an Ordered Series of Events Culminating in Membrane Permeabilization by Bax

Jonathan F. Lovell,[1] Lieven P. Billen,[1] Scott Bindner,[1] Aisha Shamas-Din,[1] Cecile Fradin,[1,2] Brian Leber,[1,3] and David W. Andrews[1,*]
[1]Department of Biochemistry and Biomedical Sciences
[2]Department of Physics and Astronomy
[3]Department of Medicine
McMaster University, Hamilton, Ontario L8N 3Z5, Canada
*Correspondence: andrewsd@mcmaster.ca
DOI 10.1016/j.cell.2008.11.010

SUMMARY

In normal circumstances, the Bcl-2 family dutifully governs when cells die. However, the rules of engagement between the pro- and antiapoptotic family members are still contested, and how Bax is transformed from a cytosolic monomer to an outer mitochondrial membrane-permeabilizing oligomer is unclear. With fluorescence techniques and an in vitro system, the combination of tBid and Bax produced dramatic membrane permeabilization. The membrane is not a passive partner in this process beause membranes are required for the protein-protein interactions to occur. Simultaneous measurements of these interactions revealed an ordered series of steps required for outer membrane permeabilization: (1) tBid rapidly binds to membranes, where (2) tBid interacts with Bax, causing (3) Bax insertion into membranes and (4) oligomerization, culminating in (5) membrane permeabilization. Bcl-XL prevents membrane-bound tBid from binding Bax. Bad releases tBid from Bcl-XL, restoring both tBid binding to Bax and membrane permeabilization.

INTRODUCTION

The Bcl-2 family of proteins function as central regulators of apoptosis in mammals and includes proteins that both up- and downregulate apoptosis. Most evidence suggests that the small regions with similar amino acid sequences shared between family members, referred to as Bcl-2 homology regions 1–4 (BH regions) mediate direct interactions between family members and that these interactions are critical to how the proteins function. The multi-BH region proteins, Bax and Bak, control commitment to apoptosis by regulating *m*itochondrial *o*uter *m*embrane *p*ermeabilization (MOMP) (Wei et al., 2001). Despite extensive study, how the Bcl-2 family proteins regulate MOMP remains speculative (Chipuk and Green, 2008). In some systems, activation of Bax for MOMP depends on proapoptotic proteins like PUMA, Bim, or a truncated fragment of Bid (tBid) that are similar only in that they contain a BH3 region (Kim et al., 2006). Direct interactions of both tBid and Bim with Bax have been reported (Marani et al., 2002), and they formed the basis for the "direct activation" model, in which BH3-only proteins activate Bax and/or Bak, leading to MOMP. In this model, a complex network of sensitizer and inhibitor proteins that act on different family members adds an additional level of regulation (Certo et al., 2006). However, a competing model suggests that a fraction of the Bax in cells is constitutively active but held in check by binding to antiapoptotic Bcl-2 family proteins (Willis et al., 2007). In this "indirect activation" model, BH3-only proteins function exclusively by binding to antiapoptotic Bcl-2 proteins, releasing Bax, and the importance of direct activation of Bax by BH3 proteins is discounted. However, both tBid and Bax independently interact with and undergo conformational changes at membranes (Wei et al., 2001; Yethon et al., 2003), and membrane-bound Bax has been reported to recruit cytoplasmic Bax to membranes (Tan et al., 2006). The importance of these interactions is emphasized in the "embedded together" model, which also includes features of both the direct and indirect activation models (Leber et al., 2007). Because there are few direct experimental data for the interactions of these proteins in membranes and a paucity of kinetic data, the relative importance, order, and mechanism(s) of many of these interactions remain unknown.

It has long been recognized that multiregion Bcl-2 proteins share structural features with α-helical pore-forming proteins; nevertheless, no consensus has emerged for the molecular mechanism of membrane permeabilization. For Bax, the process involves at least three steps: migration to membranes, insertion into the lipid bilayer, and oligomerization. However, the order of these events is unsettled. Indeed, a priori, there is no reason why the events leading to MOMP need occur in a specific order. Although it is generally agreed that BH3-only proteins promote Bax-mediated membrane permeabilization, the underlying mechanism(s) remains contentious. Experiments using soluble protein domains and peptides have failed to demonstrate productive interactions between BH3-only proteins and Bax (Willis et al., 2007), whereas in other studies, membrane

permeabilization in cells, isolated mitochondria, or liposomes by full-length Bax usually depends upon addition of either a BH3 protein or peptide (Kuwana et al., 2002; Billen et al., 2008). An important difference between these experimental approaches is inclusion in the latter of a lipid bilayer in the form of a liposome or isolated cellular membrane. Thus, the minimum components required in vitro for membrane permeabilization include Bax, an activator protein, and a lipid membrane. Multiple approaches have been used to unravel the mechanism of Bax activation, including surface plasmon resonance (Kim et al., 2005), glycosylation mapping (García-Sáez et al., 2004), and mutagenesis (Wang et al., 1998). However, during the course of Bax activation by BH3 proteins such as tBid, it is still not known whether (1) membrane binding plays a role in tBid function, (2) Bax activation occurs in the cytosol or at the membrane, and (3) the putative direct interaction between tBid and Bax is essential for MOMP. To examine the molecular mechanism by which Bax permeabilizes membranes requires a system in which the individual molecular events can be analyzed in isolation. For this reason, cell-free systems are useful to allow individual interactions of the relevant proteins to be examined with greater clarity (Basanez and Hardwick, 2008). Cell-free systems recapitulate the characteristic Bax traits observed in apoptotic cells—namely, Bax migration to membranes (Wolter et al., 1997) and oligomerization (Antonsson et al., 2001). Since it is not clear that all of the interacting components have been identified, rather than use isolated mitochondria and cell extracts we used purified proteins and liposomes. The use of a purified system allows the core mechanism to be addressed while avoiding complications from other known and unknown proteins, metabolites, and posttranslational modifications that may contribute additional levels of regulation. To ensure that our system reports as authentically as possible on the different protein-protein and protein-membrane interactions that result in membrane permeabilization, we used full-length wild-type proteins or functional single cysteine mutants of Bax. We attached low molecular weight fluorescent dyes to either endogenous or engineered cysteine residues in proteins or within the acyl chains of the lipids to follow molecular interactions using Förster resonance energy transfer (FRET), or by measuring changes in the spectral properties of the dyes reflective of changes in the hydrophobicity of their environment. In this way, it was possible both to recapitulate Bax-mediated membrane permeabilization and to measure in real time the various protein-protein and protein-membrane interactions involved.

Our results suggest that membrane permeabilization depends upon an ordered series of conformation changes and protein-protein and protein-membrane interactions initiated by membrane binding of tBid. Conformational changes in both tBid and Bax resulting from their interaction with membranes greatly increase the rate and extent of tBid-Bax binding. Moreover, the direct binding of tBid to Bax occurs on the membrane and is followed by integration of Bax into the bilayer and recruitment of additional Bax. Subsequent oligomerization of Bax results in the formation of pores in membranes, with substoichiometric quantities of tBid remaining associated with the pore and Bax oligomerization continuing even after membranes are permeabilized. Bcl-XL inhibits the process by binding to and sequestering membrane-bound tBid. Bad releases tBid from Bcl-XL and the released tBid molecules bind to and activate Bax.

RESULTS AND DISCUSSION

To quantify membrane permeabilization, we measured the release of four fluorescent molecules encapsulated together in liposomes. Because each of the molecules has distinct excitation and emission spectra, it was possible to measure the release of all four molecules in the same samples. The encapsulated molecules included both low molecular weight compounds (methoxypyrenetrisulfonic acid trisulfonate [MPTS], 0.45 kDa, and fluorescein conjugated dextran, 3 kDa) and large fluorescent proteins (allophycocyanin [APC], 100 kDa, and B-phycoerythrin [BPE], 250 kDa). As expected, when the membranes were intact, the encapsulated molecules cofractionated with the liposomes in the excluded volume by Sepharose CL-2B gel filtration chromatography (Figure 1A, fractions 1–7). After incubation with 20 nM tBid and 200 nM Bax, the fluorescent molecules were released from liposomes and, therefore, eluted in later fractions (Figure 1A, right panel, fractions 8–22). During gel filtration chromatography, the released fluorescent dextran eluted in earlier fractions than expected on the basis of the molecular weight of the polymer, presumably because of some nonspecific binding of the dextran to the liposomes (Heuck et al., 2003). However, this released fraction and that of the large proteins (fractions 8–15) were still clearly resolved from intact liposomes (fractions 1–7). Fluorescence spectroscopy was used to quantify the different fluorophores in each of the fractions for three experiments (Figure 1B). Liposomes were not permeabilized by 200 nM Bax (Figure 1B) or 20 nM tBid alone (data not shown). When both tBid and Bax were present, release of all four fluorophores increased as the concentration of Bax increased from 25 nM to 200 nM. Thus, in incubations containing tBid, Bax, and membranes in proportions roughly similar to those seen in cells, the two proteins permeabilized liposomes and released proteins as large as 250 kDa. This assay clearly demonstrates that tBid and Bax are sufficient to permeabilize liposome membranes.

Similar to observations in cells, tBid activates Bax to bind to and permeabilize membranes in vitro (Kuwana et al., 2002; Billen et al., 2008). However, it is unclear whether membrane binding of Bax and Bax oligomerization to form pores are coordinated or separately regulated processes, or whether the reaction proceeds as an ordered series of events or stochastically. When Bax binding to membranes and oligomerization was measured by gel exclusion and gel filtration chromatography, respectively (Figure S1 available online), the experiments provided rather poor temporal resolution. Although consistent with Bax membrane binding preceding Bax oligomerization, these data cannot rule out a stochastic process in which both processes occur concurrently. Furthermore, oligomerization and membrane permeabilization cannot be directly correlated via this approach. The formation of detergent-resistant oligomers provides only an indirect measure of Bax-Bax interactions in membranes, and the detergents required to solubilize the membrane may have unanticipated effects on protein-protein interactions. Crosslinking has been used as an independent method to assess interactions of these proteins, although the temporal

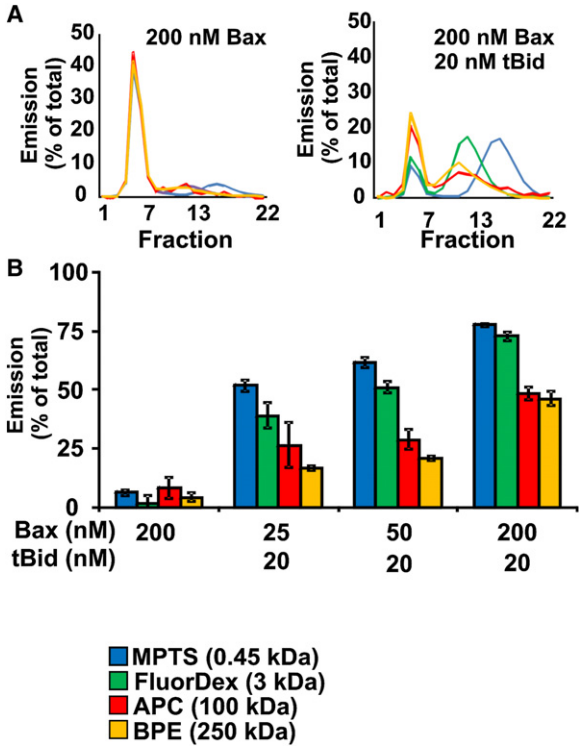

Figure 1. Bax and tBid Are Jointly Required for the Permeabilization of Liposomes

(A) Chromatograms from gel filtration columns of liposome encapsulated fluorophores of various sizes (MPTS [0.45 kDa], blue; fluorescein dextran [3 kDa], green; APC [100 kDa], red; BPE [250 kDa], yellow). All four fluorophores were encapsulated in the same liposomes and remained encapsulated when incubated with Bax (left panel) but were released from liposomes incubated with tBid and Bax (right panel). Superposition of the curves in the left panel results in only the yellow curve being visible for the main peak. Liposomes eluted in the excluded fractions (1–7) while released proteins separated in the included fractions (8–21).

(B) Release of fluorophores from liposomes quantified for three experiments such as those shown in (A) demonstrates that membrane permeabilization increases with increasing concentrations of Bax and releases proteins of up to 250 kDa. Error bars indicate the standard deviation, n = 3.

resolution is even more problematic (Billen et al., 2008). Therefore, to observe these events in real time, we examined tBid-Bax and Bax-Bax interactions and the interactions of these proteins with membranes by fluorescence techniques.

Bax Binds tBid Only if Membranes Are Present

Binding of Bax to tBid was examined with FRET between dimethylaminocoumarin (DAC)-labeled tBid and 7-nitrobenzene-2-oxa-1, 3-diazol-4-yl ethylenediamine (NBD)-labeled Bax. For these experiments murine tBid was labeled on the one endogenous cysteine (residue number 126 of Bid) with DAC; this protein was designated DAC-tBid. DAC is a blue-emitting coumarin derivative that is a good energy transfer donor for the acceptor dye NBD (Förster radius ~5 nm). As an acceptor, a single cysteine version of Bax was constructed by changing cysteine 62 to alanine, and the protein was labeled on the remaining endogenous cysteine (position 126) with NBD; this protein was designated NBD-126-Bax. After they were labeled, both proteins retained similar activity to the unlabeled, wild-type proteins in a dye release assay for membrane permeabilization (Figure S2). As a negative control, tBid with a mutation in the BH3 region, tBid G94E, previously shown not to bind Bax (Wang et al., 1996), was substituted for DAC-tBid. As expected, when incubated with Bax and liposomes, neither tBid G94E nor DAC-tBid G94E induced significant dye release (Figure S2).

When DAC-tBid (20 nM) and NBD-126-Bax (100 nM) were incubated together, energy transfer (detected as a decrease in donor fluorescence) was observed only if membranes (~2.5 nM liposomes) were also present (Figure 2A), suggesting that the two proteins interact only when bound to membranes. Consistent with this interpretation, substitution of DAC-tBid G94E for DAC-tBid significantly ($p < 0.05$) reduced the energy transfer with NBD-126-Bax. However, although both DAC-tBid and the DAC-tBid G94E point mutant bound membranes very efficiently (see below), DAC-tBid G94E did not trigger the membrane insertion of NBD-126-Bax (data not shown). It therefore remains possible that the FRET we observed between DAC-tBid and NBD-126-Bax was due to their proximity in the membrane bilayer rather than resulting from a specific interaction. To address this possibility, we added 50 μM Bid BH3 peptide to NBD-126-Bax and liposomes prior to the addition of either DAC-tBid G94E or DAC-tBid. At these concentrations, the Bid BH3 peptide has been shown to trigger insertion of Bax into membranes (Henderson et al., 2007) and result in membrane permeabilization (data not shown).

The minimal FRET observed between DAC-tBid G94E and NBD-126-Bax was not affected by preincubation with Bid BH3 peptide, suggesting that proximity in the membrane bilayer itself does not account for the FRET observed between DAC-tBid and NBD-126-Bax. The residual FRET may instead be due to residual binding between the proteins not detected by coimmunoprecipitation. However, if that was the case, then we would expect the FRET to be further reduced by the addition of excess BH3 peptide, which would compete with DAC-tBid G94E for binding to Bax. Consistent with direct binding between DAC-tBid and NBD-126-Bax, addition of the Bid BH3 peptide reduced the energy transfer between DAC-tBid and NBD-126-Bax (Figure 2B). Taken together, these results confirm that the FRET observed between DAC-tBid and NBD-126-Bax resulted from a specific interaction in the membrane bilayer and was not due merely to proximity based on their colocalization.

The extent of energy transfer between DAC-tBid and NBD-126-Bax did not decrease over time (Figure 2A), suggesting that at steady state some fraction of tBid remained bound to Bax in the lipid membrane. This result was unexpected given that tBid and Bax do not cofractionate when liposomes or mitochondria are solubilized with the detergent CHAPS (Billen et al., 2008). Unlike nonionic detergents such as Triton X-100, CHAPS does not artificially promote interactions between Bcl-2 family proteins (Hsu and Youle, 1997). When 2% CHAPS was added to the incubations containing tBid, Bax, and liposomes, it reduced the interaction between tBid and Bax measured by FRET (Figure 2B, +det.). Thus, although tBid bound Bax in membranes, most of the heteromers dissociated when the membrane was solubilized with CHAPS.

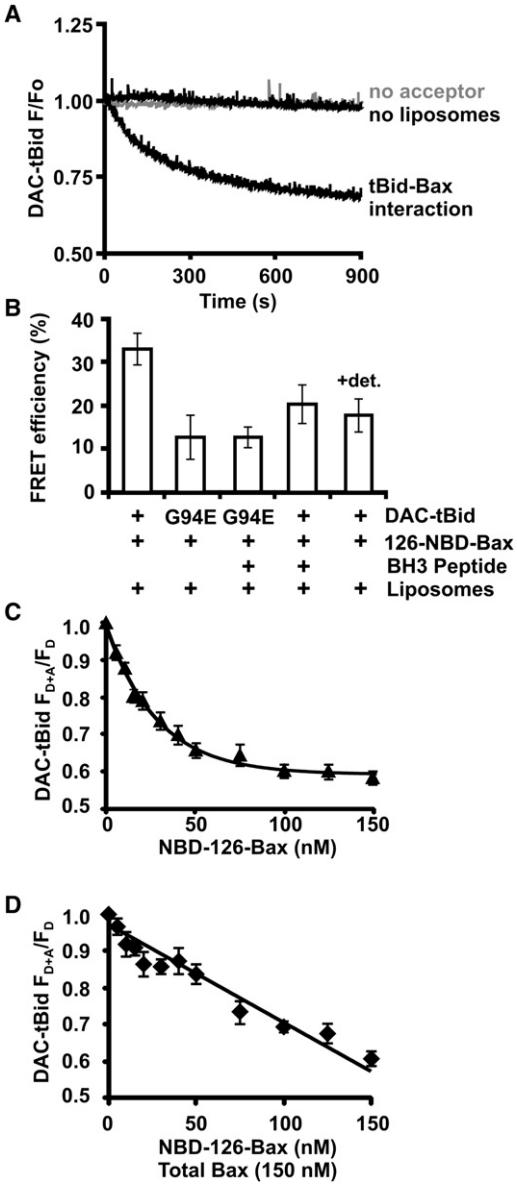

Figure 2. tBid Binding to Bax Requires Membrane

(A) DAC-tBid (20 nM) fluorescence decreases because of FRET with NBD-126-Bax (100 nM) only when liposomes (125 μM lipid) are present. In incubations without the NBD acceptor on Bax or without added liposomes, the fluorescence of DAC-tBid does not decrease. F/Fo is the fluorescence at the indicated time divided by the fluorescence at time zero.

(B) FRET was measured from pairs of reactions containing liposomes (125 μM lipid), 20 nM DAC-tBid (tBid), or DAC-tBid G94E (G94E) with either unlabeled 100 nM Bax to measure fluorescence of the donor (F_D) or 100 nM NBD-126-Bax to measure fluorescence of the donor with acceptor (F_{D+A}). FRET efficiency ($1-F_{D+A}/F_D$) was quantified after incubation for 30 min. BH3 peptide: 50 μM Bid BH3 peptide was used to trigger Bax to insertion into the liposome membrane for 2 hr prior to the addition of DAC-tBid. The addition of 2% CHAPS at the end of the incubation (+det.) reduces tBid binding to Bax measured as FRET between DAC-tBid and NBD-126-Bax. Error bars indicate the standard error, n = 8–12. The FRET efficiency for DAC-tBid and NBD-126-Bax was significantly higher ($p < 0.05$, ANOVA) than that for any of the other samples. There were no significant differences between the other samples.

Detection of FRET between DAC-tBid and NBD-126-Bax at steady state allowed examination of the concentration dependence of the interaction at equilibrium. As expected for an authentic interaction, binding of NBD-126-Bax to DAC-tBid was saturable (Figure 2C). The decrease in DAC-tBid fluorescence in samples prepared containing different amounts of NBD-126-Bax was fit with a single exponential, resulting in an apparent Kd of ~20 nM. This value must be interpreted with caution because there are a number of underlying assumptions for which there is no evidence, including that the interaction is bimolecular and that the subunits are exchangeable. As a partial test of the latter assumption, samples were prepared in which the total amount of Bax was 150 nM but the amount of NBD-126-Bax varied (Figure 2D). Consistent with the subunits being exchangeable, the resulting binding data fit better to a straight line than to an exponential decay. Although the r^2 value for the linear fit was only 0.95, there was too much variation within the data (note that the error bars are standard error for n = 7–9) to justify more sophisticated curve fitting. Taken together, these data strongly suggest that when bound to membranes there is a direct but reversible binding interaction between tBid and Bax.

tBid Binds to Membranes Rapidly

Our results suggest that interaction of tBid and/or Bax with the membrane is prerequisite for heterodimerization. Because tBid and Bax have each been reported to interact with membranes independently in a variety of systems, we examined each putative interaction separately. To measure tBid binding to liposomes, we incubated DAC-tBid with liposomes labeled by including 0.5% w/w 1-Oleoyl-2-[12-[(7-nitro-2-1,3-benzoxadiazol-4-yl) amino]dodecanoyl]-sn-Glycero-3-Phosphoethanolamine (NBD-PE). Comparison of the DAC fluorescence for DAC-tBid bound to liposomes with and without NBD-labeled lipids revealed energy transfer between DAC-tBid and NBD-labeled lipids (Figure 3A). Most of the decrease in DAC fluorescence occurred within the first 4–6 s required to add and mix the tBid into the reaction therefore fluorescence of the DAC-tBid donor alone (F_D) was estimated from a parallel incubation without NBD-labeled lipids. All of the tBid in the incubation bound to liposomes sufficiently tightly that it was recovered in membrane-containing fractions after gel filtration chromatography (data not shown). Therefore, it was possible to use the decrease in DAC fluorescence and the amount of labeled tBid in the reaction to calculate that during the first 10 s of incubation, the rate at which tBid bound to membranes was at least 10^{12} molecules/s. As a control for random collisions between the fluorescently labeled protein and membranes, we repeated the reaction with DAC-HisBid

(C) Binding of NBD-126-Bax to DAC-tBid is saturable. End point assays (2 hr) are shown for FRET between 20 nM DAC-tBid liposomes (125 μM lipid) and the indicated concentration of NBD-126-Bax. FRET data (F_{D+A}/F_D) were fit to a simple exponential decay. Error bars indicate the SEM for n = 7–9.

(D) Subunit exchange in complexes of DAC-tBid and NBD-126-Bax. Binding between 20 nM DAC-tBid liposomes (125 μM lipid) and the indicated concentration of NBD-126-Bax were allowed to come to equilibrium (2 hr) as in (C), and then unlabeled Bax was added to bring the final concentration of Bax to 150 nM. FRET between DAC-tBid and NBD-126-Bax was measured as in (C). The data were fit with a straight line of best fit. Error bars indicate the SEM for n = 7–9.

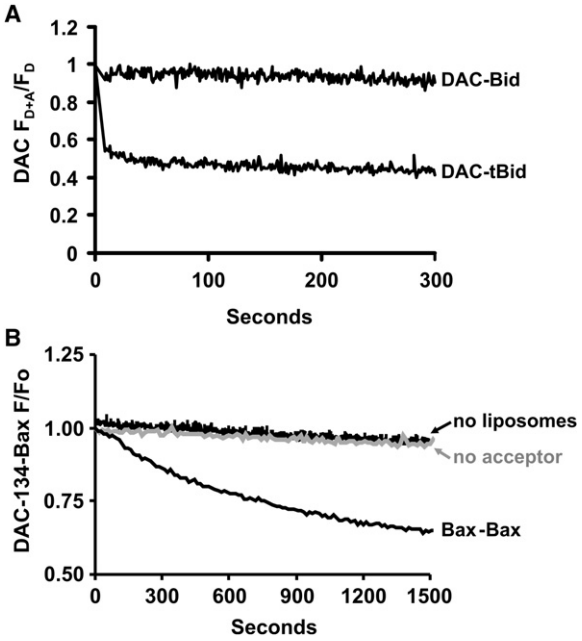

Figure 3. Binding of tBid to Liposomes and Bax Oligomerization Measured by FRET

(A) tBid binds to membranes very rapidly. Fluorescence of DAC-tBid or DAC-HisBid (DAC-Bid) after incubation with liposomes containing NBD-PE (F_{D+A}) and without NBD-PE (F_D) for the indicated time is shown. F_{D+A}/F_D is the fluorescence at the indicated time of the donor in incubations containing both donor and acceptor divided by the fluorescence of the donor a similar incubation without the acceptor. The decrease in F_{D+A}/F_D indicates that FRET between DAC-tBid and NBD-PE in the liposomes resulting from tBid binding to liposomes.

(B) Bax oligomerization measured as FRET between DAC-134-Bax and NBD-126-Bax. The fluorescence of DAC-134-Bax at the indicated time (F) divided by the fluorescence of DAC-134-Bax immediately upon addition of NBD-126-Bax (Fo) is shown for the conditions indicated: without liposomes (no liposomes), with Bax instead of NBD-126-Bax (no acceptor), and with NBD-126-Bax and DAC-134-Bax (Bax-Bax). Wild-type tBid (20 nM) was present in all reactions. The decrease in F/Fo indicates FRET due to DAC-134-Bax binding to NBD-126-Bax.

instead of DAC-tBid. Full-length Bid does not bind tightly to membranes, and consequently no significant FRET was observed between the DAC-HisBid and NBD liposomes (Figure 3A). Taken together, these results demonstrate that tBid binding to liposomes is very rapid. Finally, this assay was also used to demonstrate that the G94E mutation in tBid did not alter DAC-tBid-G94E binding to membranes (Figure S3).

In contrast with tBid, published data suggest that Bax interacts only weakly with liposome membranes (Yethon et al., 2003) and mitochondria (Billen et al., 2008) unless it is activated. Although transient, the interaction results in a change in the conformation of Bax that can be detected with a conformation-specific antibody or by crosslinking. Consistent with the low-affinity and transient nature of the interaction between Bax and liposomes, only a small amount of FRET was detected between DAC-labeled Bax and NBD liposomes. However, the interaction was too small to easily differentiate binding from collisions in solution, making it difficult to estimate either the initial rate or steady-state fraction of Bax bound to the membrane (data not shown).

Bax-Bax Interaction

In the presence of membranes, Bax behaves as a monomer by gel filtration chromatography (Yethon et al., 2003), yet Bax monomers undergo a conformational change that can be detected via intermolecular crosslinking with DSS (Billen et al., 2008), suggesting that Bax molecules are frequently in close enough proximity that the chemical can react with multiple monomers. However, these approaches (e.g., Figure S1) lack the temporal resolution to determine where in the sequence of molecular events leading to membrane permeabilization Bax oligomerizes. To examine this issue by measuring FRET, we labeled Bax monomers with either the donor (DAC) or acceptor (NBD) and then mixed them together.

Energy transfer was not detected for 20 nM DAC-134-Bax and 100 nM NBD-126-Bax in incubations that did not contain liposomes even when tBid was included (Figure 3B). However, fluorescence from DAC-134-Bax decreased slowly in incubations containing both tBid (20 nM) and liposomes (2.5 nM), consistent with oligomerization of Bax requiring both an activator and a membrane (Figure 3B). No change in DAC fluorescence was observed in control reactions containing DAC-134-Bax, tBid, and liposomes but containing unlabeled Bax instead of NBD-126-Bax (Figure 3B, no acceptor), confirming that the decrease in DAC fluorescence resulted from energy transfer from DAC-134-Bax to NBD-126-Bax in Bax oligomers.

Membrane Permeabilization Results from a Series of Ordered Reactions

The FRET data for 20 nM DAC-134-Bax and 100 nM NBD-126-Bax suggest that Bax oligomerization takes place on a very different time scale than tBid binding to membranes (compare Figures 3A and 3B). Thus, the reactions of tBid and Bax may be ordered rather than occurring stochastically. Although our results clearly demonstrate that tBid binding to membranes occurs prior to any of the other interactions that contribute to membrane permeabilization, ordering the other steps from separate experiments is less certain. The fraction of tBid bound to Bax in membranes at equilibrium is not known. Similarly, the fraction of Bax undergoing FRET at the end of the incubation is unknown. Therefore, it was not possible to calculate absolute values for the rates of tBid-Bax or Bax-Bax oligomerization. To examine the order of events in more detail, we established an assay in which it was possible to make three measurements from a single incubation. As shown schematically, in one incubation, tBid binding to Bax (Figure 4A, I), Bax insertion into membranes (Figure 4A, II) and membrane permeabilization (Figure 4A, IV) were measured. In another incubation Bax-Bax interaction (Figure 4A, III), Bax insertion into membranes and membrane permeabilization were measured.

Measuring multiple events in a single sample was feasible by selecting appropriate fluorophores and optimizing selection of excitation and emission wavelengths. DAC fluorescence was measured by excitation at 380 nm and emission at 460 nm, leaving most of the visible spectrum available for additional fluorescence measurements. The fluorescent dye NBD is not only

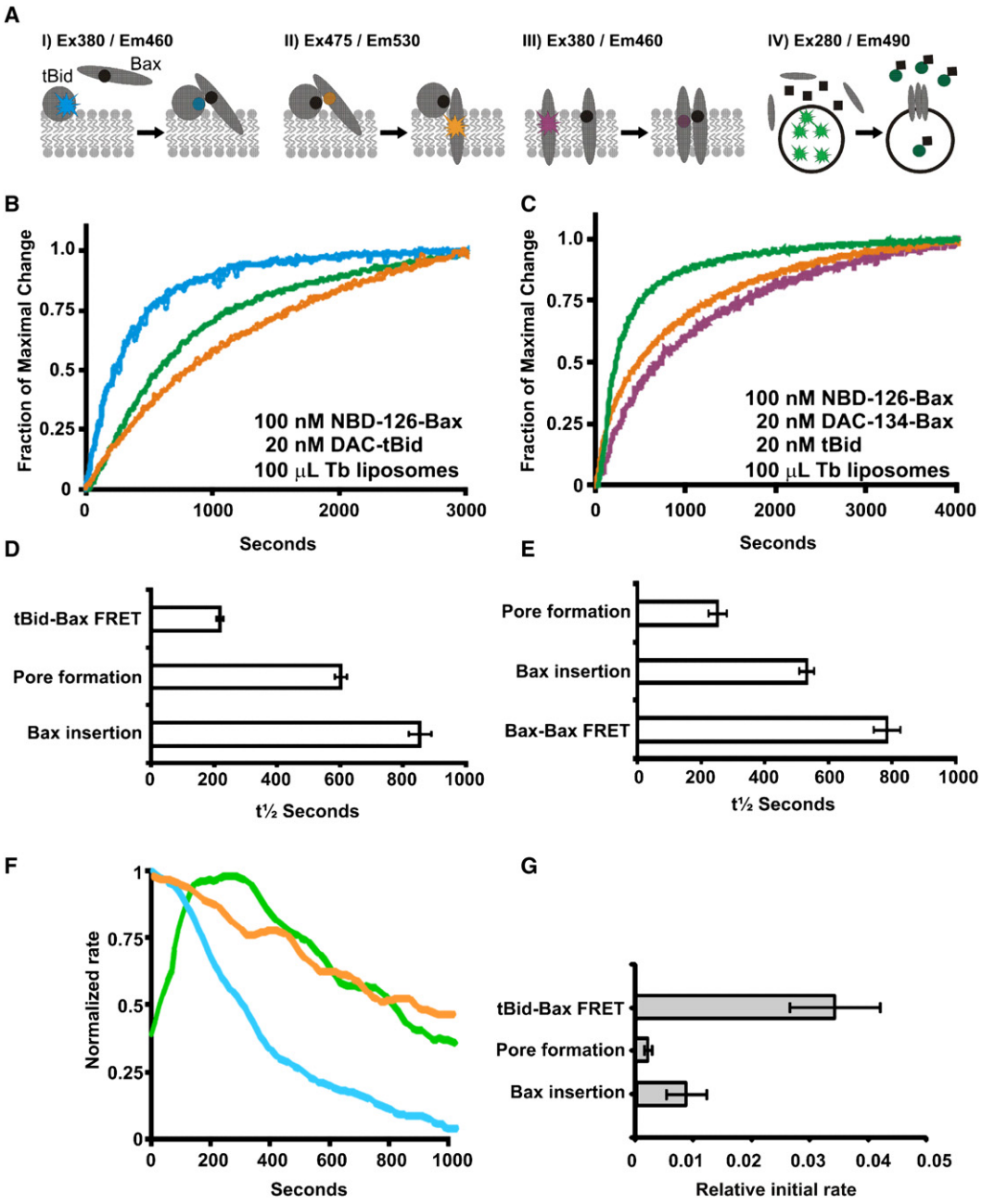

Figure 4. tBid Binding to Membranes Initiates an Ordered Series of Conformational Changes Leading to Membrane Permeabilization by Bax

(A) Fluorescence-based assays for tBid binding to Bax (I), Bax inserting into the membrane (II), Bax oligomerization (III), and membrane permeabilization (IV). Excitation (Ex) and emission (Em) wavelengths are indicated in nm.

(B) Time courses for tBid binding to Bax (cyan), membrane permeabilization (green), and Bax insertion into membranes (orange) expressed as a fraction of the maximal change for incubations containing the indicated components.

(C) Time courses for membrane permeabilization (green), Bax insertion into membranes (orange), and Bax oligomerization (purple) expressed as a fraction of the maximal change for incubations containing the indicated components.

(D and E) Time to 50% completion for the indicated reactions quantified for three replicates of the experiments in (B) and (C), respectively.

(F) Initial rates of the reactions in (B) normalized to the maximum rate for each.

(G) Relative initial rates for the first 15 s for the reactions in (B).

Error bars in (D), (E), and (G) indicate the standard deviation, n = 3.

a good acceptor for DAC fluorescence, but it can also be used to monitor insertion of a protein into a lipid bilayer because the fluorescence intensity of NBD increases when the dye moves to a more hydrophobic environment (Shepard et al., 1998). The two measurements can be made in the same incubation because the absorbance of NBD at wavelengths shorter than 480 nm that are critical for energy transfer from DAC is minimally affected by the environment of the dye. Insertion of Bax into the membrane was monitored by illuminating the sample at 475 nm and measuring the increase in fluorescence emission of the NBD-126-Bax at 530 nm. Finally, liposome permeabilization was measured by loading liposomes with a terbium-dipicolinic acid complex. This highly fluorescent complex (excitation 280 nm, emission 490 nm selected to minimize interference between the assays) is efficiently quenched by chelating the terbium with EDTA. Because the EDTA was added to the medium outside the liposomes, membrane permeabilization was required for the EDTA to chelate the terbium and quench the fluorescence (Heuck et al., 2003). Through recording of all three measurements every 15 s, it was possible to follow three reactions in a single incubation over the same time course (Figure 4).

After the terbium-dipicolinic acid complex is encapsulated, the liposomes must be separated from the nonencapsulated dye by gel filtration chromatography. As a result, the concentration of liposomes is difficult to control precisely, and it is both lower and more variable in these reactions than in those described above (Figures 2 and 3). Moreover, the total amount of Bax used in the experiment in Figure 4B is less than that in the experiment in Figure 4C. For all of these reasons, the absolute values of the reactions cannot be compared between independent experiments. However, the relative ordering of reactions within a single incubation is accurate both qualitatively and quantitatively.

To facilitate visual comparison of the data, we show changes in fluorescence (energy transfer from DAC to NBD, fluorescence increase for NBD, and fluorescence decrease for terbium dipicolinic acid) as a fraction of the maximal change. In this way, each reaction was scaled between 0 (the starting point) and 1 (the end point). When this approach was used to examine tBid binding to Bax, Bax insertion into the membrane, and membrane permeabilization, it appeared that tBid bound to Bax as a separate step that occurred prior to either Bax insertion into the membrane or membrane permeabilization (Figure 4B). This was assessed quantitatively by comparison of the $t_{1/2}$ for the reactions for three replicates of the experiment (Figure 4D). Although Bax continued to insert into membranes for more than 3000 s (Figure 4B), by this point, more than 90% of the Bax added to the reaction had embedded in the membrane (data not shown). The amount of time required for the last 10% of the NBD-126-Bax to insert into membranes does not affect the $t_{1/2}$ of the reaction.

In multiple independent experiments, the $t_{1/2}$ for tBid-Bax FRET was always substantially less than that for Bax insertion into membranes or membrane permeabilization. These results are consistent with tBid binding to Bax being a separate step that occurs prior to insertion of Bax into membranes. However, in our experimental system, 20 nM tBid results in almost complete insertion of 100 nM Bax (Figure S1A) and as shown in Figure 2, some fraction of tBid remains bound to Bax in the liposome membrane. Another explanation for these data is that once Bax inserts into membranes, the membrane-bound Bax continues to recruit soluble Bax to the membrane, thereby extending the half-time for insertion of Bax into membranes. It is therefore possible that binding of tBid to Bax may occur at the same time as insertion of the tBid bound Bax into the membrane, while the integration into membranes of soluble Bax recruited by membrane bound Bax (or the tBid-Bax complex) occurs afterwards. To minimize the potentially confounding effect of Bax recruiting Bax to the membrane on the measured $t_{1/2}$ of the reaction and further resolve the order of events, we compared the initial rates for the relevant reactions (Figures 4F and 4G, described in more detail below).

In complementary but independent experiments in which Bax-Bax FRET was measured, both membrane permeabilization and insertion of Bax into the membrane were accelerated compared to Figure 4B. As noted above, there may be several reasons for this variability. Nevertheless, the ordering of the two processes was the same in multiple independent experiments, and Bax-Bax FRET always tracked with or slightly behind Bax insertion into membranes. As a result, the $t_{1/2}$ for Bax insertion into the membrane was less than that for Bax-Bax FRET (Figure 4E). These data strongly suggest that the interaction that results in FRET between DAC-134-Bax and NBD-126-Bax occurs shortly after Bax inserts into membranes. Thus, at least one step in the Bax oligomerization process occurs after Bax inserts into membranes.

Ordering the individual steps from the data in Figures 4B and 4C relative to membrane permeabilization is complicated because quenching of the terbium dipicolinic acid complexes begins and ends before Bax-Bax binding has come to equilibrium and before all of the Bax has inserted into membranes. Nevertheless, visual inspection of the change in DAC-tBid fluorescence due to FRET with NBD-126-Bax compared to quenching of terbium-dipolinic acid suggested that tBid binds to Bax much more rapidly than membrane permeabilization (Figure 4B). This is consistent with the measured $t_{1/2}$ for the reaction and suggests that tBid-Bax binding is not rate limiting in membrane permeabilization. It may seem counterintuitive that the $t_{1/2}$ for membrane permeabilization is less than that for either Bax insertion into membranes or oligomerization. However, it is likely the result of Bax continuing to insert into and oligomerize in the bilayer of liposomes that have already been permeabilized. Our assay measures only the initial permeabilization of each liposome, because once the terbium-dipicolinic acid has been released, subsequent permeabilization events in that liposome cannot be detected. Therefore, to compare the relative rates of the different interactions with membrane permeabilization, we measured them at early times, when the contribution of further oligomerization "events" on the overall rate of the reaction could be neglected. When initial rates are compared (Figures 4F and 4G), it is clear that during the first 15 s, membrane permeabilization is much slower than either Bax insertion into membranes or oligomerization. This is consistent with models in which more than one Bax protein must insert into a liposome to permeabilize it.

To permit initial rates to be displayed graphically for all three interactions, we normalized them such that the maximum rate for each was set to 1. Although the rate of membrane

permeabilization is shown for the first 1000 s of the incubation, it is likely that more than half of the permeabilization events occur in liposomes that have not previously been permeabilized only prior to the previously measured $t_{1/2}$ of 600 s. Therefore, to follow changes in permeabilization rates, we considered only the first ~300 s of the reaction. Consistent with oligomers of Bax mediating membrane permeabilization, the rate remained lower than the maximum rate for more than 150 s. The maximum rate for permeabilization occurred at the time when tBid-Bax binding was coming to equilibrium (Figure 4B), suggesting that once a critical threshold of Bax inserted into the bilayer, permeabilization occurred rapidly. As expected, the rate of permeabilization began to decline prior to the $t_{1/2}$ because Bax continued to accumulate in the membranes of liposomes that had already been permeabilized and inserted into and permeabilized intact liposomes.

The examination of initial rates also permits us to determine whether tBid binds Bax as a separate interaction prior to insertion of Bax into membranes. As above, the change in fluorescence during the first 15 s of each reaction was used to estimate the initial rate. To permit comparison of the initial rates for the different interactions, we expressed each as a fraction of the total reaction per second. During the first 15 s of the incubation, the initial rate for Bax insertion into membranes should not be affected by Bax recruiting additional Bax proteins, because the amount of Bax in the membrane is negligible compared to the amount of membrane bound tBid (Figure 3). The initial rate data demonstrate that tBid binding to Bax preceded both insertion of Bax into the membrane and pore formation by Bax (Figure 4G). The rate of tBid binding to Bax then dropped relatively rapidly (Figure 4F), as expected, since there was much less tBid (20 nM) in the reaction than Bax (100 nM) and half of the tBid that binds to Bax at equilibrium was bound in just over 200 s. These results strongly suggest that tBid binding to Bax is a separate step that precedes insertion of Bax into the bilayer. Moreover, they suggest that a step subsequent to tBid binding to Bax is rate limiting for membrane permeabilization.

When the initial rates were compared for Bax-Bax interaction and Bax insertion into membranes, the difference in the two rates was smaller than the variation in the rates between independent experiments. However, in every experiment, Bax oligomerization occurred relatively rapidly after insertion of Bax into the membrane (e.g., Figure 4C). The simplest explanation for these results is that insertion of Bax into the lipid bilayer (Figure 4A, step II) is the rate-limiting step. The identification of this specific change in Bax as rate limiting for the entire process has important implications because it suggests that insertion of Bax into the membrane is a potential therapeutic target. Taken together, our results indicate that once tBid binds to membranes, permeabilization proceeds in the order illustrated in Figure 4A (steps I–IV).

Regulation of tBid-Bax Interactions by Bcl-XL and Bad

We have recently shown that Bcl-XL inhibits Bax-mediated membrane permeabilization by competing with Bax for binding to tBid and Bax (Billen et al., 2008). However, for purification of tBid, the full-length Bid protein was first digested with caspase 8, and then the p7 fragment was separated from the p15 fragment with octyl-glucoside. One possible implication of the need for this detergent-based separation step is that release of the cBid p7 fragment from the active cBid p15 fragment in cells is protein mediated and therefore may be tightly regulated, as proposed previously (Tait et al., 2007; Zha et al., 2000). However, when assayed both for binding to membranes by FRET and for triggering Bax to permeabilize liposomes by dye release, His-tagged cBid was as effective as tBid (Figure S4). Furthermore, separation of the p7 and p15 fragments of cBid occurred spontaneously upon addition of liposomes, as determined by FRET between each fragment and the membrane (Figure S4). Addition of DAC-126-cBid (DAC-labeled cBid in which the cysteine in the p7 fragment was replaced by serine and the endogenous cysteine at position 126 was labeled with DAC) to liposomes resulted in rapid formation of DAC-126-cBid p15 (data not shown). The DAC fluorophore is in the same position in DAC-126-cBid as in the DAC-tBid used above. As expected, DAC-126-cBid triggered Bax-mediated release of liposome contents in a manner inhibitable by Bcl-XL (Figure S4). Addition of Bcl-XL did not inhibit DAC-126-cBid from binding membranes, but it did prevent it from binding to NBD-126-Bax (Figures S4 and S5). Together, these results strongly suggest that membrane binding is sufficient to separate the two fragments of cBid, and therefore a separate cBid activating protein is not required. We conclude, therefore, that our cell-free system includes all of the essential core components for regulating membrane permeabilization.

There are two competing models for the mechanism by which Bcl-XL prevents membrane permeabilization. In one model, the primary interaction is sequestration of BH3-only region proteins such as cBid p15, whereas the other model suggests that Bcl-XL binds to and inhibits Bax. A prediction of the former model that distinguishes it from the latter is that BH3 only proteins such as Bad release cBid p15 from Bcl-XL, and the released cBid p15 molecules then bind to and activate Bax. Although there is substantial indirect evidence for (and against) this model, it has been difficult to test directly. In particular, it is not clear whether it is cBid p15 released from Bcl-XL that activates Bax. Alternatively, other molecules of cBid p15 might activate Bax, or it might be activated some other way. To test the hypothesis that cBid p15 molecules released from Bcl-XL by Bad bind to and activate Bax directly, we used fluorescence spectroscopy to monitor binding of DAC-126-cBid to NBD-126-Bax and insertion of NBD-126-Bax into the bilayer as above. In these assays, it was possible to visualize both processes in real time from a single incubation directly from the fluorescence traces.

Binding of cBid p15 to Bax was monitored by measuring the decrease in DAC fluorescence due to FRET when DAC-126-cBid binds to NBD-126-Bax (Figure 5A), while insertion of NBD-126-Bax into the liposome membrane was monitored by the increase in NBD fluorescence that accompanies movement of the dye to a more hydrophobic environment, which we interpret as insertion of the dye into the lipid bilayer (Figure 5B). Background fluorescence, primarily due to scatter from the lipsomes, is seen in both traces prior to the addition of DAC-126-cBid. As expected, when DAC-126-cBid was added to the reaction, there was an equivalent large increase in fluorescence (Ex 380 nm/ Em 460 nm) whether or not the incubations also contained Bcl-XL. Subsequent addition of NBD-126-Bax to the incubations that

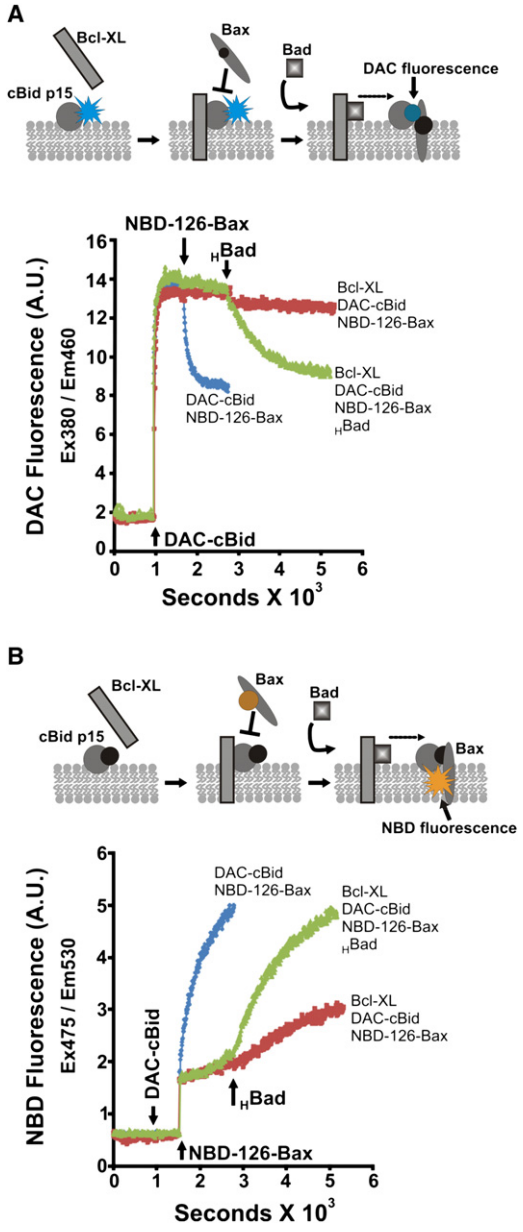

Figure 5. Bcl-XL-Mediated Inhibition of DAC-cBid p15 Binding to NBD-126-Bax Is Relieved by $_H$Bad

DAC-cBid binding to NBD-126-Bax results in FRET detected as decreased DAC-fluorescence (Ex380/Em460) (A) and insertion of Bax into the membrane detected as increased NBD-fluorescence (Ex475/Em530) (B). Background signal was measured for incubations containing liposomes (blue line) or liposomes and 40 nM Bcl-XL (green and red lines), and then the other proteins were added at the times indicated by the arrows: DAC-cBid (20 nM), NBD-126-Bax (100 nM), and $_H$Bad (400 nM). Unprocessed fluorescence traces (arbitrary units) are shown for a single experiment representative of three independent experiments.

did not contain Bcl-XL resulted in a substantial decrease in the fluorescence of DAC-126-cBid due to FRET resulting from binding of the two proteins in the membrane (Figure 5A, blue line). Consistent with DAC-cBid functioning similarly to tBid, the rate of change and the extent of FRET was similar to that seen for DAC-tBid and NBD-126-Bax (Figure 4B). As expected, the interaction of DAC-126-cBid and NBD-126-Bax was effectively blocked by Bcl-XL (Figure 5A, red line). Addition of full-length His-tagged Bad ($_H$Bad) restored binding of DAC-126-cBid to NBD-126-Bax, as seen by the decrease in DAC fluorescence over time due to FRET (Figure 5A, green line). At the concentrations of the proteins used here, essentially all of the DAC-126-cBid p15 bound to Bcl-XL prior to the addition of Bad (Billen et al., 2008 and data not shown). Therefore, our FRET data demonstrate that the DAC-126-cBid p15 molecules released from Bcl-XL by $_H$Bad proceed to bind to Bax.

Measurements of NBD fluorescence from the same samples confirmed that binding of DAC-126-cBid to NBD-126-Bax triggered Bax to insert into liposomes (Figure 5B, blue line). However, when 40 nM Bcl-XL was present in the sample, Bax insertion into the membrane was largely inhibited for 30 min. Addition of $_H$Bad restored Bax insertion into membranes with kinetics similar to cBid-mediated insertion of NBD-126-Bax in the absence of Bcl-XL, demonstrating that 400 nM $_H$Bad was sufficient to completely inhibit the function of 40 nM Bcl-XL. However, even in the absence of Bad, 40 nM Bcl-XL did not completely prevent insertion of NBD-126-Bax into the bilayer, especially after extended times (>30 min, Figure 5B), even though membrane permeabilization was effectively blocked (Figure S4). We presume that the Bax that inserts into the membrane is bound by Bcl-XL and thereby prevented from oligomerizing, as seen previously (Billen et al., 2008). The data shown are from a single experiment representative of three independent experiments quantified in Figure S6. Taken together, our results establish that cBid-p15 molecules released from Bcl-XL by $_H$Bad rapidly bind to and activate Bax, causing it to insert into liposome membranes, where Bax then oligomerizes and permeabilizes the membrane.

In cells and in cell-free reactions, arguably the most abundant component of the permeabilization process is the membrane. Nevertheless, the membrane has been generally considered a passive recipient of Bcl-2 family proteins. The ordered reactions that we have elucidated for tBid initiated Bax-mediated membrane permeabilization take place primarily in and on the lipid membrane. Moreover, the membrane contributes actively to the process by inducing conformation changes in the proteins requisite for membrane permeabilization.

By reconstituting the entire process of activation, recruitment to membranes, permeabilization, inhibition by Bcl-XL, and release from inhibition with Bad, we have demonstrated the functional relationships underlying the core molecular mechanism by which Bcl-2 family proteins regulate membrane permeabilization. We have shown that, contrary to several current models, the events are regulated by reversible binding interactions with sufficiently different rates to result in an ordered stepwise mechanism. Our results are consistent with a model in which regulation is achieved via modulation of this series of competitive binding interactions by expression levels, localization, interactions with other known and unknown proteins, posttranslational modifications of the proteins, and changes in the lipids in the outer mitochondrial membrane (Billen et al., 2008, Leber et al., 2007). The core molecular mechanism of MOMP revealed here

provides a framework by which these regulatory mechanisms can be identified and evaluated. In addition, the series of assays devised here will be useful in the elucidation of the molecular mechanisms by which other proteins and small molecules that interact with Bcl-2 family proteins regulate apoptosis.

EXPERIMENTAL PROCEDURES

Protein Purification and Labeling

For expression and purification of the mutants of Bax with a single cysteine at position 126 or 134, the corresponding cDNAs were transferred from the appropriate retroviral vectors (Annis et al., 2005) into the IMPACT bacterial expression system (New England Biolabs), generating plasmids pMAC1731 and pMAC1736, respectively. Recombinant Bax was purified as described previously (Yethon et al., 2003). Plasmids encoding His-Bid G94E (pMAC2121) and His-Bid C30S (pMAC2118) were generated from the His-Bid-encoding plasmid (pMAC1446) with Quikchange mutagenesis (Stratagene). His-Bid, tBid, C30S Bid, C126S Bid, the caspase-8 cleavage products, and the corresponding G94E proteins were purified as described (Dlugosz et al., 2006). Details of the purification of the other proteins, labeling reactions, and fluorescence spectroscopy are provided in the Supplemental Data.

For the liposome permeabilization assays in Figure 1, 1 mg mitochondrial-like lipids (0.46 mg egg phosphatidylcholine, 0.25 mg egg phosphatidylethanolamine, 0.11 mg bovine liver phophatidylinositol, 0.10 mg 18:1 phosphatidylserine, and 0.08 mg cardiolipin) were hydrated in Buffer A (10 mM HEPES [pH 7], 135 mM KCl, 1 mM $MgCl_2$). For incorporation of MPTS, (0.75 mM, Anaspec #85725), 3 kDa fluorescent dextran (0.5 mg, Invitrogen #D3305), APC, (0.4 mg, Cyanotech #100300), and BPE, (0.4 mg, Cyanotech #100301), they were added to lipid films in 1 ml of Buffer. Liposomes were formed by extrusion, and unincorporated dyes and fluorescent molecules were removed by gel filtration over a 12 ml Sepharose CL-2B column equilibrated with Buffer A. After incubation with the indicated proteins in a 300 μl reaction, released fluorophores were separated from permeabilized liposomes by gel filtration with 3 ml Sepharose CL-2B column and collecting 300 uL fractions. CHAPS was added to all fractions to 1% in order to eliminate self-quenching in unlysed liposomes before quantification with fluorescence.

SUPPLEMENTAL DATA

Supplemental Data include Supplemental Experimental Procedures and six figures and can be found with this article online at http://www.cell.com/supplemental/S0092-8674(08)01439-6.

ACKNOWLEDGMENTS

This work was supported by grant FRN12517 from the Canadian Institute of Health Research (CIHR) to D.W.A. and B.L. and a Tier I Canada Research Chair in Membrane Biogenesis to D.W.A. L.P.B. is recipient of a CIHR Canada Graduate Scholarship.

Received: June 22, 2008
Revised: September 15, 2008
Accepted: November 4, 2008
Published online: December 4, 2008

REFERENCES

Annis, M.G., Soucie, E.L., Dlugosz, P.J., Cruz-Aguado, J.A., Penn, L.Z., Leber, B., and Andrews, D.W. (2005). Bax forms multi-spanning monomers that oligomerize to permeabilize membranes during apoptosis. EMBO J. *24*, 2096–2103.

Antonsson, B., Montessuit, S., Sanchez, B., and Martinou, J.C. (2001). Bax is present as a high molecular weight oligomer/complex in the mitochondrial membrane of apoptotic cells. J. Biol. Chem. *276*, 11615–11623.

Basanez, G., and Hardwick, J.M. (2008). Unravelling the Bcl-2 apoptosis code with a simple model system. PLoS Biol. *6*, 1148–1151.

Billen, L.P., Kokoski, C.L., Lovell, J.F., Leber, B., and Andrews, D.W. (2008). Bcl-XL inhibits membrane permeabilization by competing with Bax. PLoS Biol. *6*, 1268–1280.

Certo, M., Moore, V.D.G., Nishino, M., Wei, G., Korsmeyer, S., Armstrong, S.A., and Letai, A. (2006). Mitochondria primed by death signals determine cellular addiction to antiapoptotic BCL-2 family members. Cancer Cell *9*, 351–365.

Chipuk, J.E., and Green, D.R. (2008). How do BCL-2 proteins induce mitochondrial outer membrane permeabilization? Trends Cell Biol. *18*, 157–164.

Dlugosz, P.J., Billen, L., Annis, M.G., Zhu, W., Zhang, Z., Lin, J., Leber, B., and Andrews, D.W. (2006). Bcl-2 changes conformation to inhibit Bax oligomerization. EMBO J. *25*, 2287–2296.

García-Sáez, A.J., Mingarro, I., Pérez-Payá, E., and Salgado, J. (2004). Membrane-insertion fragments of Bcl-XL, Bax, and Bid. Biochemistry *43*, 10930–10943.

Henderson, M.P.A., Billen, L.P., Kim, P.K., and Andrews, D.W. (2007). Cell-free analysis of tail-anchor protein targeting to membranes. Methods *41*, 427–438.

Heuck, A.P., Tweten, R.K., and Johnson, A.E. (2003). Assembly and topography of the prepore complex in cholesterol-dependent cytolysins. J. Biol. Chem. *278*, 31218–31225.

Hsu, Y.T., and Youle, R.J. (1997). Nonionic detergents induce dimerization among members of the Bcl-2 family. J. Biol. Chem. *272*, 13829–13834.

Kim, H., Rafiuddin-Shah, M., Tu, H.-C., Jeffers, J.R., Zambetti, G.P., Hsieh, J.J.-D., and Cheng, E.H.-Y. (2006). Hierarchical regulation of mitochondrion-dependent apoptosis by BCL-2 subfamilies. Nat. Cell Biol. *8*, 1348–1358.

Kim, M., Jung, S.O., Park, K., Jeong, E.-J., Joung, H.-A., Kim, T.-H., Seol, D.-W., and Chung, B.H. (2005). Detection of Bax protein conformational change using a surface plasmon resonance imaging-based antibody chip. Biochem. Biophys. Res. Commun. *338*, 1834–1838.

Kuwana, T., Mackey, M.R., Perkins, G., Ellisman, M.H., Latterich, M., Schneiter, R., Green, D.R., and Newmeyer, D.D. (2002). Bid, Bax, and lipids cooperate to form supramolecular openings in the outer mitochondrial membrane. Cell *111*, 331–342.

Leber, B., Lin, J., and Andrews, D.W. (2007). Embedded together: the life and death consequences of interaction of the Bcl-2 family with membranes. Apoptosis *12*, 897–911.

Marani, M., Tenev, T., Hancock, D., Downward, J., and Lemoine, N.R. (2002). Identification of novel isoforms of the BH3 domain protein Bim which directly activate Bax to trigger apoptosis. Mol. Cell. Biol. *22*, 3577–3589.

Shepard, L.A., Heuck, A.P., Hamman, B.D., Rossjohn, J., Parker, M.W., Ryan, K.R., Johnson, A.E., and Tweten, R.K. (1998). Identification of a membrane-spanning domain of the thiol-activated pore-forming toxin Clostridium perfringens perfringolysin O: an α-helical to beta-sheet transition identified by fluorescence spectroscopy. Biochemistry *37*, 14563–14574.

Tait, S.W., de Vries, E., Maas, C., Keller, A.M., D'Santos, C.S., and Borst, J. (2007). Apoptosis induction by Bid requires unconventional ubiquitination and degradation of its N-terminal fragment. J. Cell Biol. *179*, 1453–1466.

Tan, C., Dlugosz, P.J., Peng, J., Zhang, Z., Lapolla, S.M., Plafker, S.M., Andrews, D.W., and Lin, J. (2006). Auto-activation of the apoptosis protein Bax increases mitochondrial membrane permeability and is inhibited by Bcl-2. J. Biol. Chem. *281*, 14764–14775.

Wang, K., Yin, X.M., Chao, D.T., Milliman, C.L., and Korsmeyer, S.J. (1996). BID: a novel BH3 domain-only death agonist. Genes Dev. *10*, 2859–2869.

Wei, M.C., Zong, W.X., Cheng, E.H., Lindsten, T., Panoutsakopoulou, V., Ross, A.J., Roth, K.A., MacGregor, G.R., Thompson, C.B., and Korsmeyer, S.J. (2001). Proapoptotic BAX and BAK: a requisite gateway to mitochondrial dysfunction and death. Science *292*, 727–730.

Willis, S.N., Fletcher, J.I., Kaufmann, T., van Delft, M.F., Chen, L., Czabotar, P.E., Ierino, H., Lee, E.F., Fairlie, W.D., Bouillet, P., et al. (2007). Apoptosis initiated when BH3 ligands engage multiple Bcl-2 homologs, not Bax or Bak. Science *315*, 856–859.

Wolter, K.G., Hsu, Y.T., Smith, C.L., Nechushtan, A., Xi, X.G., and Youle, R.J. (1997). Movement of Bax from the cytosol to mitochondria during apoptosis. J. Cell Biol. *139*, 1281–1292.

Yethon, J.A., Epand, R.F., Leber, B., Epand, R.M., and Andrews, D.W. (2003). Interaction with a membrane surface triggers a reversible conformational change in Bax normally associated with induction of apoptosis. J. Biol. Chem. *278*, 48935–48941.

Zha, J., Weiler, S., Oh, K.J., Wei, M.C., and Korsmeyer, S.J. (2000). Posttranslational N-myristoylation of BID as a molecular switch for targeting mitochondria and apoptosis. Science *290*, 1761–1765.